

AUG 3 1971  
SEP 3 1971  
MAR 29 1973



# LASER DOPPLER VELOCIMETER DUAL SCATTER PROBE VOLUME

W. H. Goethert

ARO, Inc.

July 1971

Approved for public release; distribution unlimited.

**ARNOLD ENGINEERING DEVELOPMENT CENTER  
AIR FORCE SYSTEMS COMMAND  
ARNOLD AIR FORCE STATION, TENNESSEE**

PROPERTY OF U S AIR FORCE  
AEDC LIBRARY  
F40600-72-C-0003

# ***NOTICES***

When U. S. Government drawings specifications, or other data are used for any purpose other than a definitely related Government procurement operation, the Government thereby incurs no responsibility nor any obligation whatsoever, and the fact that the Government may have formulated, furnished, or in any way supplied the said drawings, specifications, or other data, is not to be regarded by implication or otherwise, or in any manner licensing the holder or any other person or corporation, or conveying any rights or permission to manufacture, use, or sell any patented invention that may in any way be related thereto.

Qualified users may obtain copies of this report from the Defense Documentation Center.

References to named commercial products in this report are not to be considered in any sense as an endorsement of the product by the United States Air Force or the Government.

LASER DOPPLER VELOCIMETER  
DUAL SCATTER PROBE VOLUME

W. H. Goethert  
ARO, Inc.

Approved for public release; distribution unlimited.

## FOREWORD

The work reported herein was sponsored by Headquarters, Arnold Engineering Development Center (AEDC), Air Force Systems Command (AFSC), under Program Element 65701F, Project 4344, Task 32.

The results of this research were obtained by ARO, Inc. (a subsidiary of Sverdrup & Parcel and Associates, Inc.), contract operator of AEDC, AFSC, Arnold Air Force Station, Tennessee, under Contract F40600-72-C-0003. The research was performed from July through October, 1970, under ARO Project BC5119, and the manuscript was submitted for publication on February 9, 1971.

The author wishes to acknowledge the assistance of Mr. T. R. Ward II for his participation on this project. In addition, the efforts of Mr. J. O. Hornkohl, a co-worker, in developing the Gaussian curve fitting relationship for the computer program as outlined in the appendix is greatly appreciated.

This technical report has been reviewed and is approved.

David G. Francis  
Captain, USAF  
Research and Development  
Division  
Directorate of Technology

Harry L. Maynard  
Colonel, USAF  
Director of Technology

## ABSTRACT

A further clarification of the volume from which data originate in the dual scatter laser Doppler velocimeter is presented. There are several factors that specify the primary dimensions of the probe volume which in some cases are totally specified by the collector optics. It was found experimentally that the lens aperture of the light collecting optics has a primary effect on the volume from which data originate. An equation is derived for reducing this data volume for both the on-axis and off-axis cases. Experimental verification is presented and compared to the derived equation.

## CONTENTS

|   | <u>Page</u> |
|---|-------------|
| ABSTRACT . . . . .  | iii         |
| I. INTRODUCTION . . . . .                                   | 1           |
| II. THEORETICAL DETERMINATION OF PROBE VOLUME<br>DIMENSIONS |             |
| 2.1 Geometric Probe Volume . . . . .                        | 1           |
| 2.2 Data Probe Volume . . . . .                             | 2           |
| 2.3 Probe Volume Determination . . . . .                    | 3           |
| III. EXPERIMENTAL VERIFICATION                              |             |
| 3.1 Beam Diameter Determination . . . . .                   | 11          |
| 3.2 Data Probe Volume Determination . . . . .               | 13          |
| IV. SUMMARY AND CONCLUSIONS . . . . .                       | 14          |
| REFERENCES . . . . .  | 17          |

## TABLE

|  |    |
|--|----|
| I. Results of Probe Volume Experiments . . . . . | 15 |
|--|----|

## APPENDIXES

## I. ILLUSTRATIONS

Figure

|  |    |
|--|----|
| 1. Experimental Data of On-Axis and Off-Axis P. V. L. . .                          | 21 |
| 2. Defining Parameters of Beam Crossover Region . . .                              | 22 |
| 3. Light Shield for Reducing Background Light Effects . .                          | 23 |
| 4. Axial Intensity versus Axial Position. . . . .                                  | 24 |
| 5. Plot of the Function $f(\phi)$ versus $\phi$ . . . . .                          | 25 |
| 6. Typical Data Plots  |    |
| a. Representative Data of Laser Beam Intensity<br>versus Radial Position . . . . . | 26 |
| b. Plot of Beam Diameter versus Distance for<br>SP-124 . . . . .                   | 27 |
| c. Intensity Plot of Diode Data with Computer<br>Curve Fit . . . . .               | 28 |

| <u>Figure</u>  | <u>Page</u> |
|--|-------------|
| 7. Automatic Diode Scan of Laser Beam Diameter for<br>SP-140 . . . . . | 29          |
| 8. Typical Setup for Off-Axis Experiments . . . . .                    | 30          |
| 9. Zero Crossing Electronic Readout . . . . .                          | 31          |
| II. GAUSSIAN CURVE FITTING . . . . .                                   | 32          |

## SECTION I INTRODUCTION

The dual scatter laser Doppler velocimeter (LDV) has been routinely used to acquire velocity information from extremely small spatial regions in flow fields. Previous attempts to accurately obtain a correlation between the experimentally deduced volume and the calculated volume have been exceedingly difficult. The experimental values obtained for probe volumes were found to be much smaller than the predicted values. This is particularly true in the case of the dual scatter, backscatter, LDV system. In this particular case, a concentric light collection system is used in conjunction with the laser beam focusing system (on-axis backscatter unit). The important aspect is that there are two distinctively separate spatial volumes under consideration. The volume defined by the two laser cross beams is termed the geometric volume; the volume associated with the light collecting optics is termed data volume. Henceforth, when reference is made to the probe volume, it is to mean the effective volume from which information is extracted with a given optical configuration. In the following discussions, all optical ray boundaries are defined as the  $1/e^2$  (0.135335...) amplitude having assumed a Gaussian curve as the amplitude distribution.

## SECTION II THEORETICAL DETERMINATION OF PROBE VOLUME DIMENSIONS

In general, probe volumes have been specified as the maximum radial diameter and the maximum axial length of the geometric probe volume defined below. This definition can be misleading where probe volumes are to be minimized when only the reduction of the geometric volume is considered. It is important not to overlook the reduction of the probe volume that is also obtained with the light collecting optics. This feature is emphatically demonstrated in Fig. 1 (Appendix I) which contains characteristic curves of the axial dimension of the probe volume obtained from an on-axis and off-axis optical arrangement coupled with an 0.018-in. aperture.

### 2.1 GEOMETRIC PROBE VOLUME

The geometric volume is formed by the intersection of the two laser cross beams. Each laser beam is focused to its minimum value at the region of intersection. Hence, since each laser beam may be described



by a Gaussian intensity distribution, the focused region may also be described by a composite Gaussian intensity distribution. The minimum focal diameter is determined for a diffraction-limited focusing system by

$$2b_o = \frac{4}{\pi} \frac{f_c}{2b} \lambda \quad (1)$$

where  $b_o$  is the radius of the focused spot,  $f_c$  the focal length of the focusing lens,  $\lambda$  the laser radiation wavelength, and  $2b$  the laser beam diameter at the focusing lens. It has been shown (Ref. 1) that three dimensions are associated with the laser beam crossover region shown in Fig. 2. These dimensions describe an ellipsoid at the  $1/e^2$  intensity points. The determination of the  $\Delta x$ ,  $\Delta y$ , and  $\Delta z$  dimensions may be easily deduced (Fig. 2) as

$$\begin{aligned} \Delta x &= 2b_o \\ \Delta y &= \frac{2b_o}{\cos \theta/2} \\ \Delta z &= \frac{2b_o}{\sin \theta/2} \end{aligned} \quad (2)$$

where  $\theta$  is the angle between the two cross beams. Nomograms have been developed (Ref. 4) that allow rapid determination of these geometric probe volume parameters.

## 2.2 DATA PROBE VOLUME

All of the velocity information is contained totally within the geometric volume; however, the data volume is only a portion of the entire geometric volume from which the velocity information is extracted.

In attempting to minimize the geometric volume, the major problem lies with the resolution of the axial dimension, or the depth of field, which is much larger than the radial dimensions; specifically, from Eq. (2)

$$\frac{\Delta z}{\Delta x} = \frac{2b_o}{\sin \theta/2} \left( \frac{1}{2b_o} \right) = \csc \theta/2 \quad (3)$$

Equation (3) indicates how much greater this dimension is compared to the (effective) diameter of the ellipsoid. A velocimeter with a 3-deg angle (typical) between beams has an axial dimension, or depth of field, 38 times greater than the effective diameter. The lens-aperture arrangement of the collector optics is one technique that may be used to reduce this axial dimension.

## 2.3 PROBE VOLUME DETERMINATION

From past experience, background light has a considerable effect on the signal-to-noise ratio of the detected Doppler-shifted frequencies. Even though efforts are generally made to reduce overhead lighting, some experiments have been set up with no consideration to overhead lighting effects. It was found that with an adequate light shield, and a black curtain placed in a suitable location, no detectable light could be measured. Figure 3 is the schematic of this setup. This experiment suggested that only light emanating from the centerline of the lens arrangement will contribute to the noise term of the velocimeter. Therefore, the effect of unfocused light on the centerline of the lens arrangement was studied also.

### 2.3.1 Theoretical Analysis, Axial Dimension

The diameter of the spot of a focused laser beam may be determined from Maxwell equations. The laser beam propagates, say, in the +z direction and spreads only by diffraction. The local direction of propagation (Ref. 2) is hyperbolic in nature, and over a spherical surface, of constant plane, the field amplitude is given by

$$E_{m,n} = E_0 \frac{r_0}{r} H_m\left(\sqrt{2} \frac{x}{r}\right) H_n\left(\sqrt{2} \frac{y}{r}\right) \exp\left(-\frac{x^2 + y^2}{r^2}\right)$$

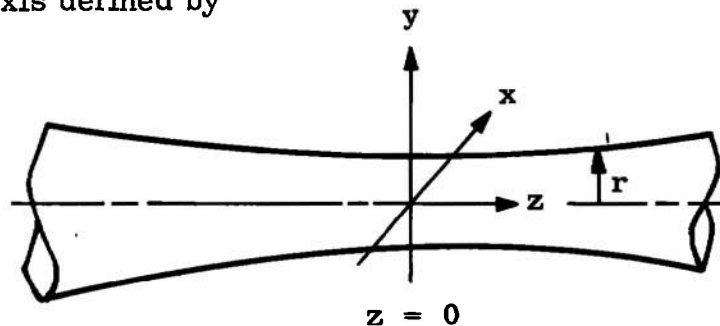
where m, n are laser modes,  $H_m$  and  $H_n$  are Hermite polynomials of order m and n,

$$r = r_0 \left[1 + \left(\frac{z}{z_0}\right)^2\right]^{1/2} \quad (4)$$

and

$$z_0 = \frac{\pi r_0^2}{\lambda}$$

and  $r_0$  is the minimum radius attainable (or the Gaussian spot) with the coordinate axis defined by



The optical arrangement of the velocimeter is such that the same lens is used for focusing the laser beams and for light collection. Since the light collecting function of the lens is characterized by a smaller  $f$ /number than the laser focusing function, we may treat the light collecting function only (since its depth of focus is considerably smaller than the laser beam focal depth). Integrating the field amplitude (Ref. 2) of the fundamental laser mode yields the power distribution as a function of radius where  $P_0$  is the total power and  $f(r)$  is some function of radius  $r$ .

$$P(r) = P_0 (1 - e^{f(r)}) \quad (5)$$

The cross-sectional area of the beam is

$$A = \pi r_o^2$$

and with the use of Eq. (4), the area ratio becomes

$$\frac{A}{A_0} = \frac{\pi \left[ r_o \sqrt{1 + \left( \frac{z}{z_0} \right)^2} \right]^2}{\pi r_o^2} = \left[ 1 + \left( \frac{z}{z_0} \right)^2 \right] \quad (6)$$

Now, since  $I = \frac{P(r)}{A}$ , where  $I$  is the intensity, we have

$$\frac{I_{axial}}{I_{max}} = [1 - e^{f(r)}] \frac{1}{\left[ 1 + \left( \frac{z}{z_0} \right)^2 \right]} \quad (7)$$

The total intensity is determined by letting  $r \rightarrow \infty$  so that  $e^{f(r)} \rightarrow 0$  and Eq. (7) becomes

$$\frac{I_{axial}}{I_{max}} = \frac{1}{\left[ 1 + \left( \frac{z}{z_0} \right)^2 \right]} = \frac{1}{\left[ 1 + \left( \frac{z\lambda}{\pi r_o^2} \right)^2 \right]} \quad (8)$$

This equation represents the axial intensity distribution where  $I_{axial}$  is the intensity at an axial distance of  $z$ . This equation was plotted in Fig. 4 for the argon laser of  $\lambda = 4880\text{\AA}$  for a variety of  $f$ /numbers where  $r_o$  was calculated with the conventional diffraction limit equation for minimum focal spot diameter;  $a$  is the lens diameter and  $L$  its focal length.

$$r_o = \frac{2}{\pi} \lambda \left( \frac{L}{a} \right) \quad (9)$$

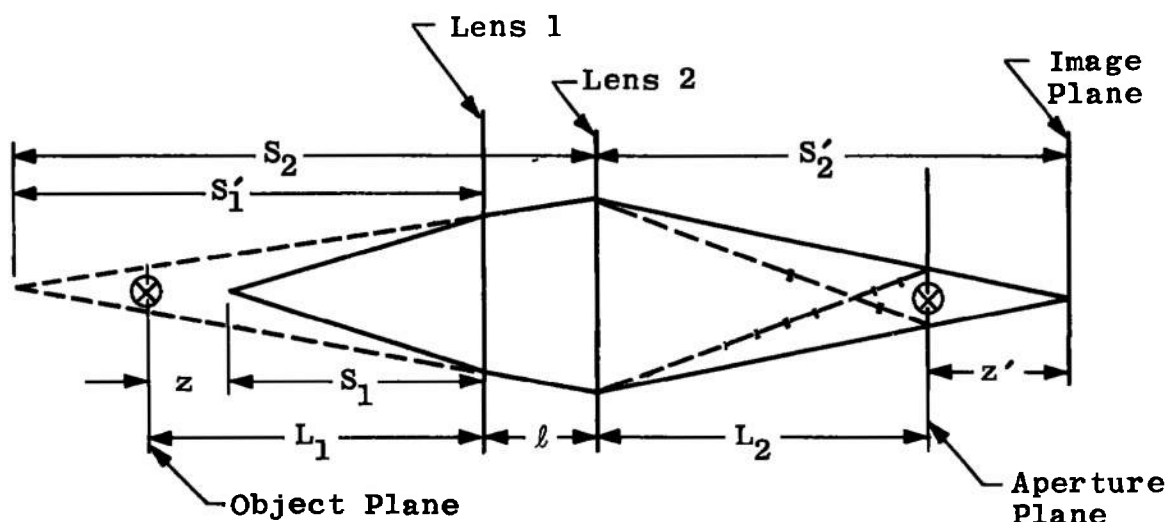
Equation (8) can also be simplified by rewriting Eq. (4) in the following manner:

$$\left(\frac{r_o}{r}\right)^2 = \frac{1}{1 + \left(\frac{z}{z_o}\right)^2} \quad (10)$$

which is identical to Eq. (8) so

$$\frac{I_{axial}}{I_{max}} = \left(\frac{r_o}{r}\right)^2 \quad (11)$$

The optical configuration of the LDV is determined by two back-to-back lenses as shown in the sketch below.



If a particle traverses the probe volume at the focal point of lens 1, the image of the scattered light falls on the aperture preceding the phototube. If the aperture is made equal to the Gaussian spot size,  $r_o$ , then the depth of the probe volume is given by Eq. (8), which provides the smallest possible axial dimension that can be achieved for a particular  $f$ /number lens. If the aperture size is larger than the  $r_o$ , a greater depth of light collection will be effected. Therefore, it will be necessary to specify the axial dimension of the probe volume in terms of the aperture preceding the phototube.

The standard thin lens equation is used to find the radius of a spot on the aperture plane in terms of light scattering particles traversing a distance  $z$  from the geometric center of the focal point. Let the focal plane of the second lens be the position where the aperture will later be located. Now, starting at the phototube end of the LDV, we can determine the shift ( $z$ ) of the image of the focal spot in terms of the  $z$  distance from the focal spot in the object plane.

Equation (4) governs  $z'$  in terms of the beam radius of both the Gaussian spot radius and any arbitrary radius of the beam at some  $z$  position. The parameters  $r_0$  and  $z_0$  may now be written in terms of the parameters of the lens configuration. Thus

$$S_2' = \frac{(\ell + |S_1'|)L_1}{(\ell + |S_1'|) - L_1} \quad (12)$$

Now,  $S_1'$  may be further written in terms of the lens 1 parameter and the  $z$  distance (that distance in the flow field that a particle may traverse off the geometric center); hence

$$S_1' = \frac{L_1(L_1 + z)}{z} \quad (13)$$

When  $L_1$  is significantly small and the distance is large, the effective beam diameter at the first lens must be taken into consideration such that  $r_{1 \text{ beam}} = \text{divergence times total image distance}$ ; so

$$r_{1 \text{ beam}} = r_{1B} = \frac{r_1}{S_1'} |S_1' + \ell| \quad (14)$$

The new value of the Gaussian spot in terms of  $S_2'$  is

$$r_0 = \frac{\lambda}{\pi r_{1B}} S_2' \quad (15)$$

Substituting into Eq. (4), we have

$$r = \frac{\lambda}{\pi r_{1B}} S_2' \sqrt{1 + \left[ \frac{\lambda}{\pi} \frac{z'}{\left( \frac{\lambda}{\pi r_{1B}} S_2' \right)^2} \right]^2} \quad (16)$$

since

$$z' = |L_2 - S_2'| \quad (17)$$

then

$$r = \frac{\lambda}{\pi r_{1B}} S_2' \sqrt{1 + \left[ \frac{\pi}{\lambda} \frac{|(L_2 - S_2')|}{S_2'^2} r_{1B}^2 \right]^2} \quad (18)$$

Equation (18) represents the radius of the image in the plane of the aperture (which is chosen to be at  $L_2$ ) in terms of the two lenses of the LDV.

From Eq. (11), the axial intensity distribution is inversely proportional to the areas of two separate diameters. Hence

$$\left(\frac{I_{\text{axial}}}{I_{\text{max}}}\right) = \left(\frac{r_{\text{AP}}}{r}\right)^2 \quad (19)$$

where  $r_{\text{AP}}$  is the chosen radius of the aperture preceding the phototube, and  $r$  the radius of the image of a particle traversing the probe volume at  $z$ . Let the axial dimension of the probe volume be defined as the  $1/e^2$  of Eq. (20) or Eq. (8); then  $z$  may be found from Eq. (17) and Eq. (20), i. e.,

$$\left(\frac{r_{\text{AP}}}{r}\right)^2 = \frac{1}{e^2} = 0.135 \quad (20)$$

or

$$\frac{r_{\text{AP}}}{0.367} = \frac{\lambda S_2'}{\pi r_{1B}} \sqrt{1 + \left(\frac{\pi}{\lambda} \frac{|L_2 - S_2'|}{S_2'^2} r_{1B}^2\right)^2} \quad (21)$$

Again,  $r_{\text{AP}}$  is the chosen aperture radius.

The total dimension is, of course,  $2z$ , since  $z$  was defined to be zero at the center or focal spot in the object plane.

Equation (21) may be approximated by assuming a linear function between the new focal spot point and the aperture plane, i. e.

$$\frac{r_{1B}}{S_2'} = \frac{r_{\text{AP}}}{z'}$$

Writing these parameters in terms of the input parameters, we have

$$r_{\text{AP}} = 0.367 \left| \frac{r_1 L_1}{S_1'} \right| \quad (22)$$

where  $r_1$  is the light collecting lens radius,  $L_1$  the light collecting lens focal point, and  $S_1'$  is given by Eq. (13). Solving Eq. (22) for the axial dimension  $z$  provides a good first-order approximation.

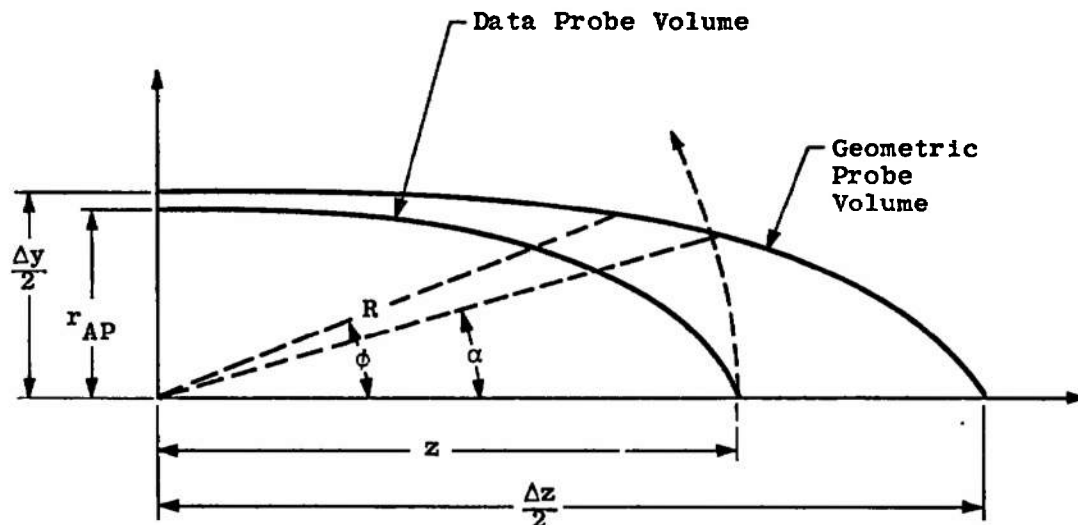
$$z \approx \frac{L_1}{\left[ 0.367 \frac{r_1}{r_{\text{AP}}} - 1 \right]} \quad (23)$$

### 2.3.2 Theoretical Analysis, Radial Dimension

The radial dimension of the data volume is the projected aperture diameter on the geometric volume. In most cases the lens arrangement is a one-to-one transfer system (no magnification) such that the aperture diameter is the diameter of the ellipsoid.

It was previously pointed out, and will be shown, that an even greater reduction in the  $z$  dimension could be effected by operating the collecting optics off axis relative to the axis of the geometric probe volume.

The geometric probe volume and the data probe volume are expressed as ellipsoids at the  $1/e^2$  intensity points. For clarity, a quarter section of each probe volume is shown in the sketch below with all symbols defined as in the above equations.<sup>1</sup>



It is evident from the sketch that the axial ( $z$ ) dimension is reduced by  $2(z \cos \phi)$  up to the angle  $\phi = \alpha$ . A further increase in  $\phi$  ( $\phi > \alpha$ ) reduces the axial dimension by

$$P.V.L. = 2(R \cos \phi) \quad (24)$$

---

<sup>1</sup>Only the cross section at  $\frac{\Delta x}{2} = 0$  will be considered since it is assumed that the volume is a symmetric ellipsoid for  $\theta < 15$  deg (see Eq. (2)).

It is, therefore, only necessary to determine  $R$  as a function of the angle  $\phi$ . At  $\phi > \alpha$ ,  $R$  varies with the geometric probe volume. The geometric probe volume is expressed in cylindrical coordinates as

$$\frac{R^2 \cos^2 \phi}{\left(\frac{\Delta z}{2}\right)^2} + \frac{R^2 \sin^2 \phi}{\left(\frac{\Delta y}{2}\right)^2} = 1 \quad (25)$$

Solving for  $R$ , we have

$$R = \frac{1}{\sqrt{\frac{\cos^2 \phi}{\left(\frac{\Delta z}{2}\right)^2} + \frac{\sin^2 \phi}{\left(\frac{\Delta y}{2}\right)^2}}} \quad (26)$$

Substituting the terms of  $\Delta z$  and  $\Delta y$  from Eq. (2),  $R$  becomes

$$R = \frac{b_0}{\sqrt{\cos^2 \phi \sin^2 \theta/2 + \sin^2 \phi \cos^2 \theta/2}} \quad (27)$$

With the use of the "power relation" trigonometric identity and multiplying, Eq. (27) reduces to

$$R = \frac{b_0}{\sqrt{\frac{1}{2}(1 - \cos \theta \cos 2\phi)}} \quad (28)$$

Equation (28) is a convenient relationship since  $R$  is expressed as a function of the laser cross beam angle,  $\theta$  and the off-axis angle,  $\phi$ .

Combining Eq. (24) with Eq. (28) gives the probe volume length as

$$\text{P.V.L.} = 2b_0 \frac{\cos \phi}{\sqrt{\frac{1}{2}(1 - \cos \theta \cos 2\phi)}} \quad (29)$$

Let

$$\frac{\cos \phi}{\sqrt{\frac{1}{2}(1 - \cos \theta \cos 2\phi)}} \equiv f(\phi) \quad (30)$$

then the length of the data probe volume becomes

$$\boxed{\text{P.V.L.} = 2b_0 f(\phi)} \quad \text{for } \phi > \alpha \quad (31a)$$

$$\boxed{\text{P.V.L.} = 2z \cos \phi} \quad \text{for } \phi < \alpha \quad (32b)$$

The function,  $f(\phi)$ , is plotted in Fig. 5 versus the angle  $\phi$  for a variety of laser cross beam angles,  $\theta$ . To use the curves in Fig. 5, it is important to calculate  $\alpha$  to determine which form of Eq. (31) to use.



At the intersection of the ellipsoid and circle, described by the rotation of the data probe volume,  $R = z$ , and  $\phi = \alpha$  (see sketch). In Eq. (28), setting  $R = z$  and solving for  $\cos 2\alpha$ , we have

$$\cos 2\alpha = \frac{z^2/2 - b_o^2}{z^2/2 \cos \theta} \quad (32)$$

Rearranging terms,  $\alpha$  is expressed as

$$\alpha = \frac{1}{2} \cos^{-1} \left[ \frac{1 - 2(b_o/z)^2}{\cos \theta} \right] \quad (33)$$

If the determination of  $\alpha$  requires the use of Eq. (31b) very little reduction is realized in the axial dimension. If the angle  $\alpha$  is very small, small off-axis angles will produce a large reduction in the length of the probe volume. A small angle  $\phi$  is easily produced by allowing the two laser beams to fall near the periphery of the focusing/collecting lens (backscatter units only), thereby allowing one to choose a very small angle  $\phi$ .

When  $\alpha$  is desired to be small, or negligible, the fraction in Eq. (33) must be made nearly equal to unity, such that  $\cos \theta \approx 1 - 2(b_o/z)^2$  or

$$\frac{b_o}{z} = \sqrt{\frac{1}{2} (1 - \cos \theta)} \quad (34)$$

Hence, one can choose which of these three independent parameters to manipulate to establish velocimeter requirements.

Equations (31a) and (31b) are applicable for off-axis angle  $\phi$ , up to approximately 20 deg since the value  $R$  is not the outermost extremity of the projected data probe volume or the geometric probe volume axis. The error involved for angles less than 20 deg is assumed to be negligible. This restriction is not serious since the trend in operational LDV units is to operate in the backscatter mode only. In this case, a 20-deg off-axis operation produces such low scattering intensities that the signal-to-noise ratio becomes too low for practical velocimeter operation. Another reason for not operating at angles greater than 20-deg is demonstrated in Fig. 5. For angles greater than 15 deg, the reduction of the P.V.L. becomes extremely small regardless of the laser cross beam angle.

## SECTION III EXPERIMENTAL VERIFICATION

### 3.1 BEAM DIAMETER DETERMINATION

It was shown (Fig. 1) that some angular relationship governs the reduction of the axial dimension of the data probe volume. The experimental curves in Fig. 1 could not be predicted theoretically. An error analysis revealed that the experimentally determined values of the phototube aperture diameter,  $2r_{AP}$ , and the laser beam diameter,  $2b$ , at the focusing lens were very sensitive to the axial data probe volume dimensions. Heretofore,  $2b$  was obtained by an intuitive guess, since accurate measurements of  $2b$  have been difficult, if not impossible, to obtain. The aperture diameter,  $2r_{AP}$ , was assumed to be circular, which generally was not the case. Also, lint or other particles sometimes blocked part of the aperture producing smaller effective aperture diameters. Therefore, an effort was directed toward the accurate measurement of the two parameters. The aperture diameter measurement problem was solved by using a microscope having a calibrated gratical in the eye piece. This permitted direct visual verification of the roundness of the aperture.

The first attempt to determine  $2b$  was to count the number of cycles of frequency information between the  $1/e^2$  points in the center of the geometric probe volume. Since  $N (1/e^2) = 4/\pi D/2b$ , where  $D$  is the two laser beam spacing before the focusing lens,  $2b$  may be calculated. It was found that this technique caused a 10-percent error in the determination of  $2b$ , hence a direct measurement was undertaken.

#### 3.1.1 Wire Technique

A method used for the direct measurement of  $2b$  was to pass a  $10\text{-}\mu$  fiber through the laser beam at a number of distances from the laser, such that the beam divergence could be determined. A fiber was then mounted on a wheel and rotated by a hysteresis-synchronous motor. Figure 6a shows a typical laser beam scan of the radial diameter. Particular notice should be given to the Gaussian shape of this fiber scan. The basic assumption of the fiber passing through the beam is that the scattering intensity of the fiber is a constant multiple times the Gaussian intensity distribution of the laser beam. To prove this, we must show that the intensity distribution of the y-axis (scan on y-axis) is Gaussian, i. e.

$$I(y) = \int_0^\infty \int_0^\infty I(r) dx dy \quad (35)$$

when

$$I(r) = ae^{-br^2}$$

since  $r^2 = x^2 + y^2$ . Substituting  $I(r)$  and  $r^2$  into  $I(y)$ , we have

$$I(y) = \int_0^\infty \int_0^{R1/e^2} ae^{-b(x^2 + y^2)} dx dy$$

or

$$I(y) = ae^{-by^2} \left( \int_0^{R1/e^2} ae^{-bx^2} dx \right) dy \quad (36)$$

The integral along the x-axis would be a constant if the integration were taken from zero to infinity. But the integration is limited to the  $1/e^2$  radius, hence Eq. (36) becomes

$$I(y) = f(y) (ae^{-by^2})$$

where  $f(y)$  is the weak function of  $y$ . Therefore,  $(y)$  is not a Gaussian function times a constant. Since  $f(y)$  is in a series form of  $(1 - ay^2 + by^4 \dots)$ , the error is small.

A series of data points taken with  $f(y)$  assumed to be constant resulted in the data shown in Fig. 6b. Several photographs were taken (Fig. 6a) at several distances from the laser. By knowing the speed of the fiber moving through the laser beam and the sweep speed of the oscilloscope, the  $1/e$  point was obtained from each photograph. (The  $1/e$  point was chosen since the background radiation affects the  $1/e^2$  intensity point more than the  $1/e$  points.) The  $1/e^2$  point was calculated by assuming a Gaussian intensity distribution. Figure 6b shows a tremendous scatter of the fiber data which cannot be readily explained with the assumption of  $f(y) = \text{constant}$ .

### 3.1.2 Aperture Technique with Phototube

To avoid the necessity of making assumptions as in section 3.1.1, an alternate technique was set up to measure the laser beam diameter versus distance. A  $10\text{-}\mu$  aperture preceding a phototube was mounted on a microdensitometer traversing table. In addition to the horizontal traverse, vertical adjustment was also incorporated such that each position in the beam could be optimized to ensure the scan was on the diameter of the beam.

The plots of the data indicated a saturation/fatigue effect after scanning through the maximum intensity. Figure 4a indicates this effect very clearly. To retain these data, a computer curve-fitting technique

(Appendix II) was applied only to the data on the fatigued side of the curve and to points approximately 10 percent over the maximum. The resulting  $1/e^2$  points are plotted in Fig. 6b.

### 3.1.3 Aperture Technique with Diode

It was believed that the light intensity passing through the  $10\text{-}\mu$  aperture would be too weak for conventional amplitude measuring devices, hence a phototube was incorporated in the measurement. Because of the fatigue/saturation problem, one datum point was taken with a photodiode. This technique requires a more elaborate experimental setup since two separate traverse units are required. The procedure followed was identical to that of the aperture phototube technique described above. Figure 6c shows the data acquired 7 ft from the laser. Included in this curve is the computer-generated curve fit which clearly shows the superiority of the technique.

Based on the diode data only, the following empirical relationship giving the beam diameter versus distance was derived for the Spectra Physics 124 laser

$$(2b \pm 0.005 = 0.11 x + 1.1)_{\text{S.P. 124}} \quad (37)$$

where  $x$  is the distance from the laser in feet, and  $2b$  is the beam diameter in millimeters.

The argon laser, Spectra Physics 140, has been the primary laser used for dual scatter LDV work. A similar equation for beam diameter versus distance would also be required. During the course of the experiment, considerable difficulty was encountered in adjusting the laser for  $\text{TEM}_{00}$  mode operation. Therefore, an automatic diode scan technique was established for rapid determination of the laser mode structure. To ensure sufficient accuracy in this determination, several scans were made at 19.5 ft. A typical scan is shown in Fig. 7. The resulting empirical relationship was determined to be

$$(2b \pm 0.05 = 0.177 x + 1.6)_{\text{S.P. 140}} \quad (38)$$

where  $x$  is in feet and  $2b$  is in millimeters.

## 3.2 DATA PROBE VOLUME DETERMINATION

Verification of Eq. (31) was effected primarily with a backscatter LDV unit. A schematic of a typical off-axis lens arrangement is shown

in Fig. 8. The on-axis experiments also used backscatter units since this eliminated the necessity of blocking the two cross beams so they would not enter the phototube. The off-axis experiments were all conducted with apertures slightly less than the  $\Delta y$  dimension of the geometric probe volume. This allowed direct comparisons between off-axis, large aperture operation and on-axis, small aperture operation. It is desirable to operate the velocimeter with large aperture because of increased signal amplitude, increased signal-to-noise ratio, more cycles in the information burst, and greater vibration tolerances. A tabulation of the data of the on-axis and off-axis experiments is included in Table I. Again,  $\phi$  is the off-axis angle. The length of the theoretical probe volume was calculated from the parameters of each experiment, and the experimental probe volume length was measured directly as described in Ref. 1. Excellent agreement can be seen in P. V. L. experiment and P. V. L. theory. It was felt that the major error of these experiments was manifested in the angle  $\phi$  because it was extremely difficult to determine.

#### SECTION IV SUMMARY AND CONCLUSIONS

It was shown in Fig. 1 that the axial dimension of the probe volume could be considerably reduced by operating the velocimeter off axis. All of the experiments were conducted with approximately the same geometric probe volume length of 0.8 in. This allows one to compare the results in Fig. 1 in relation to the relatively long probe volume length. A vital point must be remembered in the design of a velocimeter: velocity information is present in the entire geometric probe volume length, but with a lens/aperture combination or off-axis operation only a portion of the total available information is used. In many cases, operating off axis with reduced scattering intensity produces greater signal intensity and more cycles of the desired information than operating on axis with very small apertures. In general, smaller probe volume lengths are obtainable (a very desirable feature for velocity resolution) with small off-axis operation as shown in Fig. 1 and elucidated further in Fig. 5.

Figure 5 provides a good illustration of the "best possible" probe volume reduction for any off-axis angle and any beam spacing,  $\theta$ , desired for velocimeter design. It is shown that a beam spacing of greater than 15 deg would produce practically no reduction in the length of the probe volume by operating off axis. On the other hand, a tremendous reduction is seen for a beam spacing of, say, 0.5 deg and very small off-axis angles.

**TABLE I**  
**RESULTS OF PROBE VOLUME EXPERIMENTS**

| $\phi$ , deg | $2 r_{AP}$  | $\theta$ , deg | $2 h$ , mm | $2 b_o$                 | $f(\phi)$      | P.V.L. Theoretical                | P.V.L. Experimental    |
|--------------|-------------|----------------|------------|-------------------------|----------------|-----------------------------------|------------------------|
| 0.           | 0.01375 in. |                |            | ---                     | ---            | (0.377) in.<br>Eq. (23)           | 0.36 in.               |
| 0            | 165 $\mu$   |                |            | ---                     | ---            | (0.178) in.<br>Eq. (23)           | 0.188 in.              |
| 8            | 0.018 in.   | 2.67           | 1.6        | 0.0151 in.              | 7.70           | (0.107) in.<br>Aperture too large | 0.247 in.              |
| 8.5          | 465 $\mu$   | 2.633          | 1.43       | 0.426 mm                | 6.61           | (2.817 mm)<br>0.011 in.           | (2.82 mm)<br>0.01 in.  |
| 10           | 0.018 in.   | 2.62           | 1.50       | 0.02346 in.             | 5.50           | 0.129 in.                         | 0.127 in.              |
| 13           | 0.018 in.   | 2.70           | 1.3        | $0.0186 \pm 0.002$ in.  | $3.75 \pm 0.3$ | $0.0697 \pm 0.0131$ in.           | $0.073 \pm 0.004$ in.  |
| 14           | 465 $\mu$   | 2.50           | 1.14       | $0.02120 \pm 0.001$ in. | 3.839          | $0.0814 \pm 0.008$ in.            | $0.0919 \pm 0.016$ in. |

An interesting fact is borne out in Eq. (31), which shows that the probe volume length is independent of the parameters of the collector optics. Since  $\alpha$  is affected directly, care must be taken in velocimeter design not to exceed the range of  $\phi$ . Conversely, for angles less than  $\alpha$ , P. V. L. is independent of the laser cross beam parameters.

The resulting probe volume in off-axis operation is obviously not symmetrical compared to the on-axis operation, but it is felt that this is of little or no consequence since the important factor in reducing the probe volume length is velocity resolution, not symmetry.

The probe volume length is greatly affected by the electronic readout unit such that the P. V. L. may be further reduced or in some cases even increased. The only effect the electronics have on the probe volume is in the form of discrimination of, for example, amplitude ratios of the information pulse and frequency deviation. The most effective method is to use a variable electronic threshold to reject all signal amplitudes below a preset level for the axial intensity distribution of the probe volume. As much as 90-percent reduction could be effected by this method.

The acceleration of the light scattering particles passing through the data probe volume must be negligible for this method to be effective. Other effects of electronic probe volume reduction are generally unique to the type of readout used in the measurement. Two specific examples of readout effects on probe volume are worth mentioning: the spectrum analyzer and the zero crossing.

The spectrum analyzer is a common technique for providing the LDV velocity information. These analyzers display the power spectrum of the frequency (velocity) content of the data probe volume. Assuming negligible acceleration in the flow, seeded with a size distribution having a narrow variance (not too difficult to obtain in practice), discrimination is effected by recording the maximum intensity of the distribution function, since particles moving at different velocities relative to geometric center of the data probe volume produce lower amplitude signals. This type of amplitude discrimination may produce extremely small probe volume lengths, such as experiments concerned with measuring velocities through shock waves where the sudden "break" in the velocity profile could easily be determined. It was experimentally determined that a probe volume movement of 0.001 in. produced this "break" in the velocity profile. Hence, for comparison,

|                               |           |
|-------------------------------|-----------|
| Geometric probe volume length | 0.9 in.   |
| Data probe volume length      | 0.2 in.   |
| Effective probe volume length | 0.001 in. |

Another experiment using a zero crossing readout was used with the same flow and LDV unit. The zero crossing unit reads the time it takes a frequency burst to cross zero level, say, ten times. Obviously, this type of readout (in its basic form) cannot be very sensitive to amplitude discrimination; regardless of the amplitude of the information signal, a "perfect" zero crossing readout will provide the velocity information. This means that regardless of the size of the data probe volume, the readout will "read" all velocities in the geometric probe volume. This was shown experimentally to be a case with the same geometric probe volume and data probe volume as in the above example (G. P. V. L. = 0.9 in; D. P. V. L. = 0.2 in). The flow was a 0.5-in.-diam free jet having a nearly constant velocity in the core of the flow. The zero crossing readout produced the velocity distribution shown in Fig. 9 with the corresponding spectrum analyzer trace. The figure shows the mean velocity in the center of the data probe volume along with a portion of velocities in the geometric probe volume. Since the geometric probe volume is much greater than the flow field, all velocities, from zero to maximum centerline velocity, should be present. The decreasing distribution may be explained by the fact that complete independence from amplitude discrimination is not feasible in "real" electronic readout units. Hence, the shape of the velocity distribution may be explained by the near-perfect readout analogy. Needless to say, a threshold built into this readout would again recover the amplitude discrimination for obtaining very small effective probe volumes.

## REFERENCES

1. Brayton, D. B. and Goethert, W. H. "New Velocity Measuring Technique Using Dual-Scatter Laser Doppler Shift." AEDC-TR-70-205, November 1970.
2. Yariv, A. and Gordon, J. P. "The Laser." Proceedings of the IEEE, January 1963.
3. Goethert, W. H. "Balanced Detection for the Dual Scatter LDV." AEDC-TR-71-70, May 1971.
4. Mycroft, G. H. and Smith, F. H. "Nomograms for the Doppler Shift Velocimeter." AEDC-TR-71-102, June 1971.



## **APPENDIXES**

- I. ILLUSTRATIONS**
- II. GAUSSIAN CURVE FITTING**

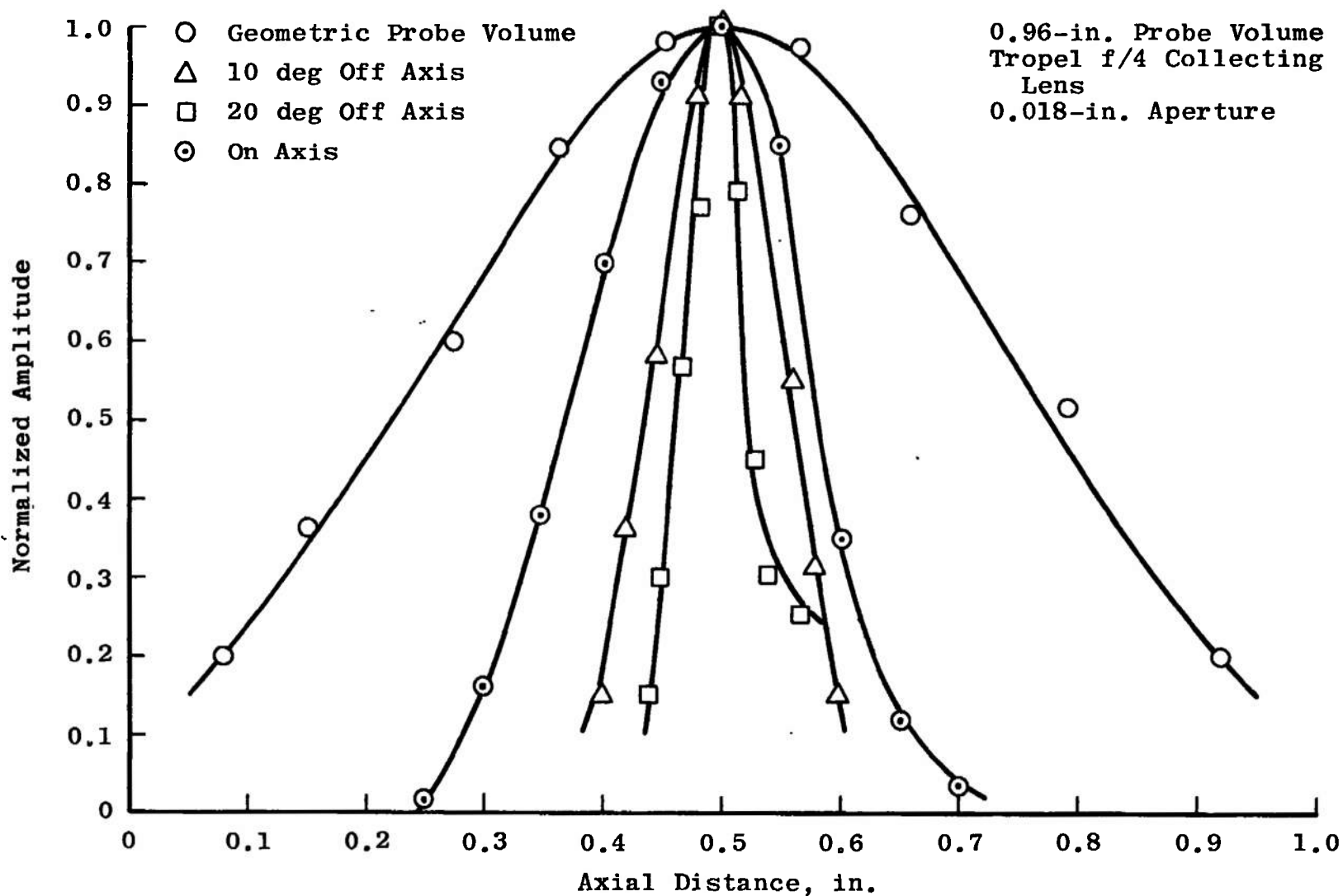


Fig. 1 Experimental Data of On-Axis and Off-Axis P. V. L.

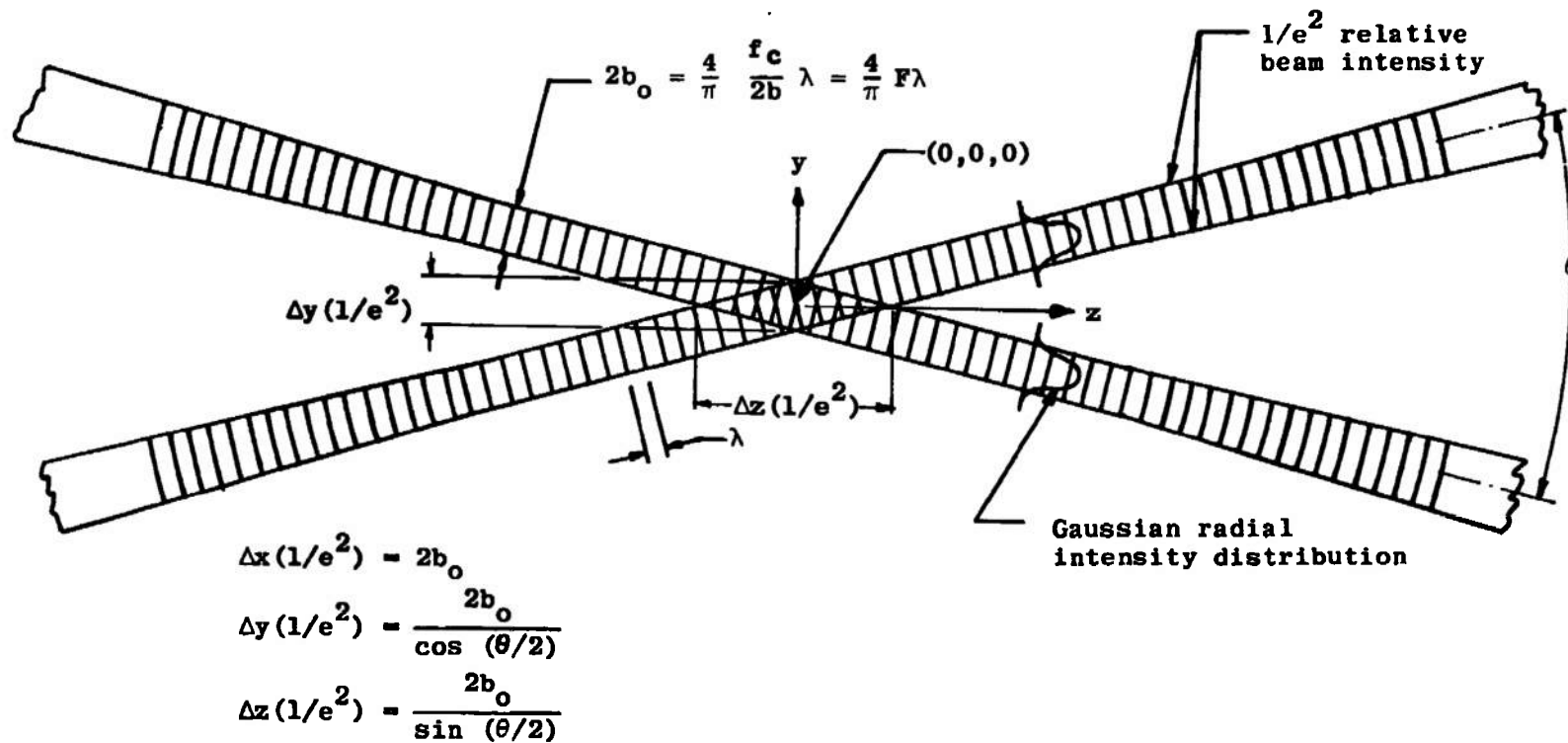


Fig. 2 Defining Parameters of Beam Crossover Region

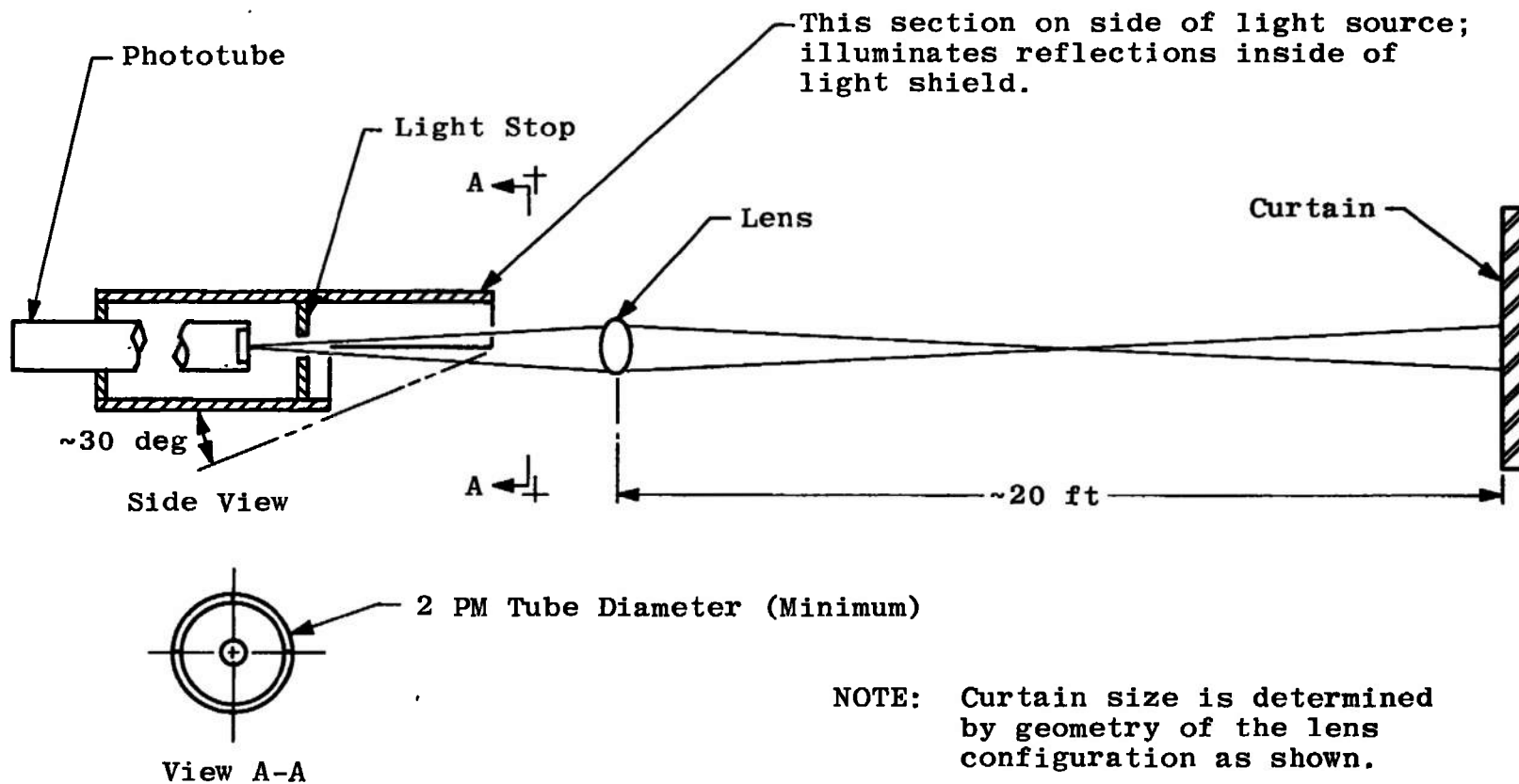


Fig. 3 Light Shield for Reducing Background Light Effects

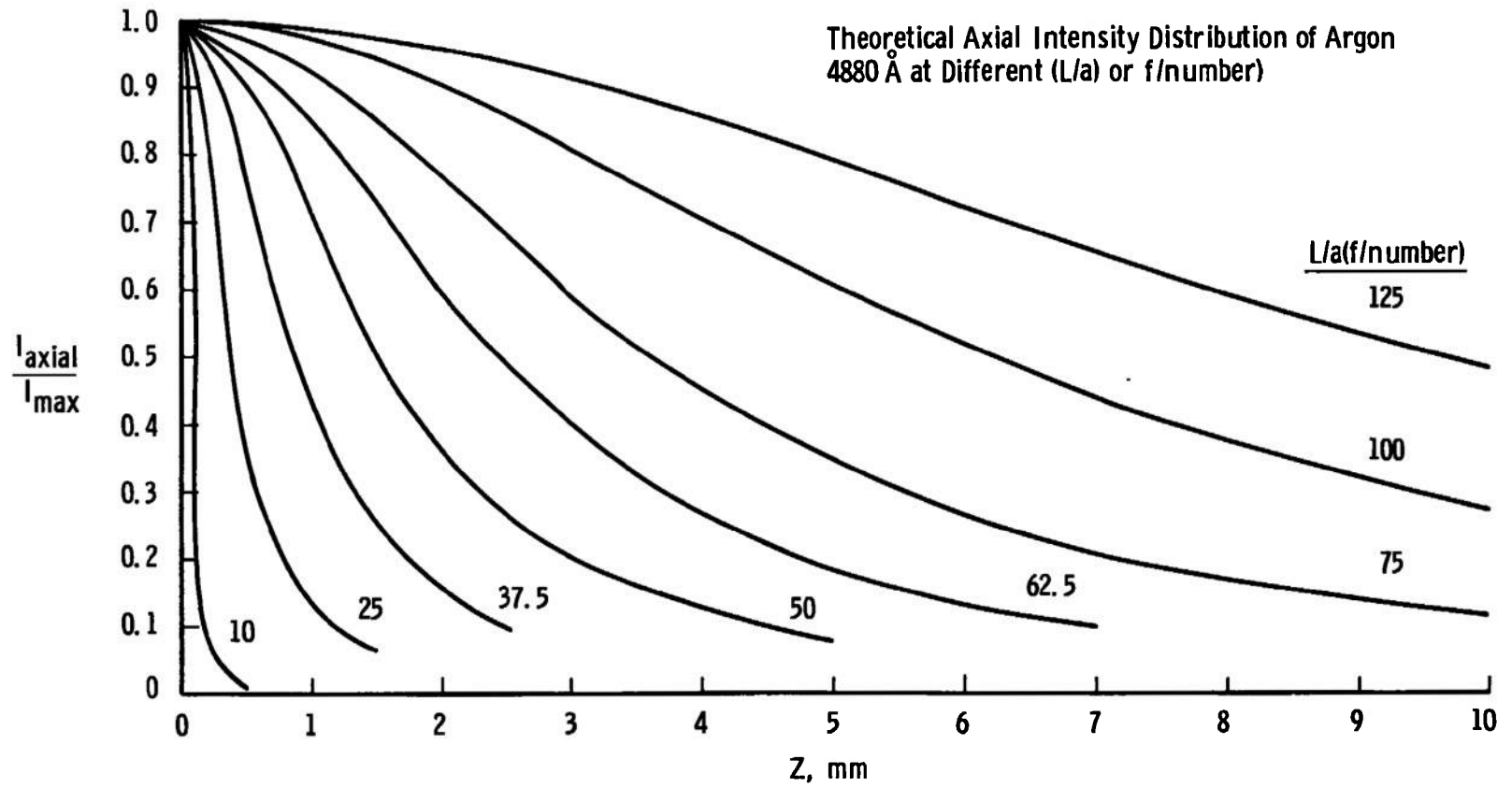
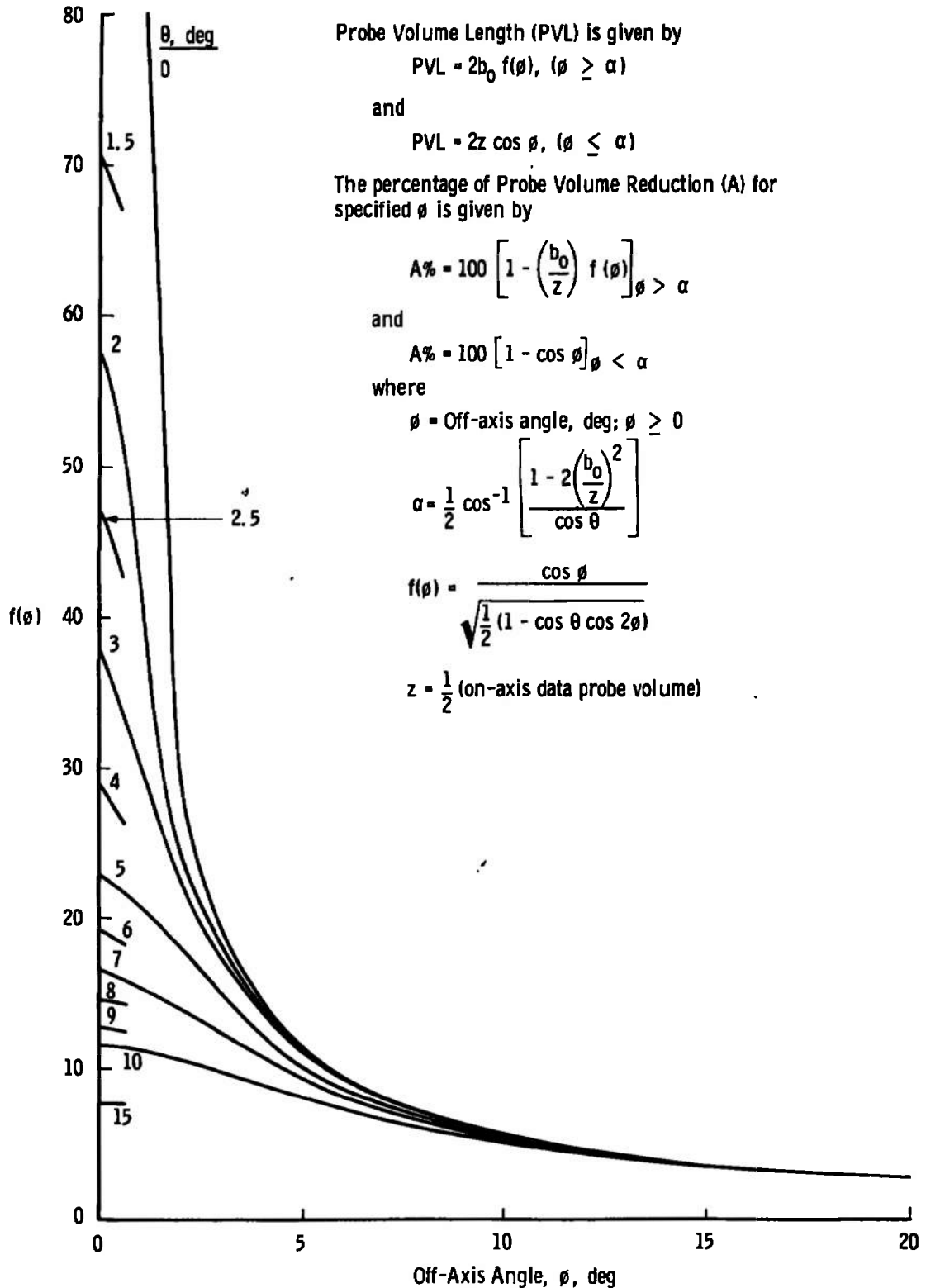
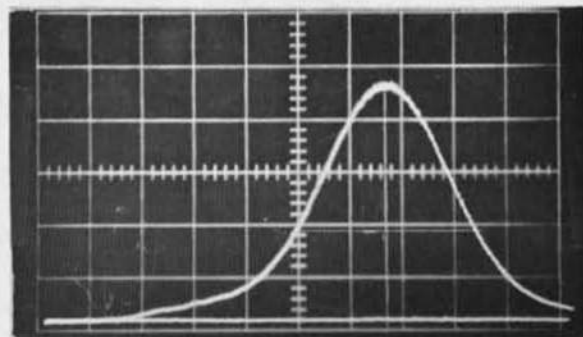
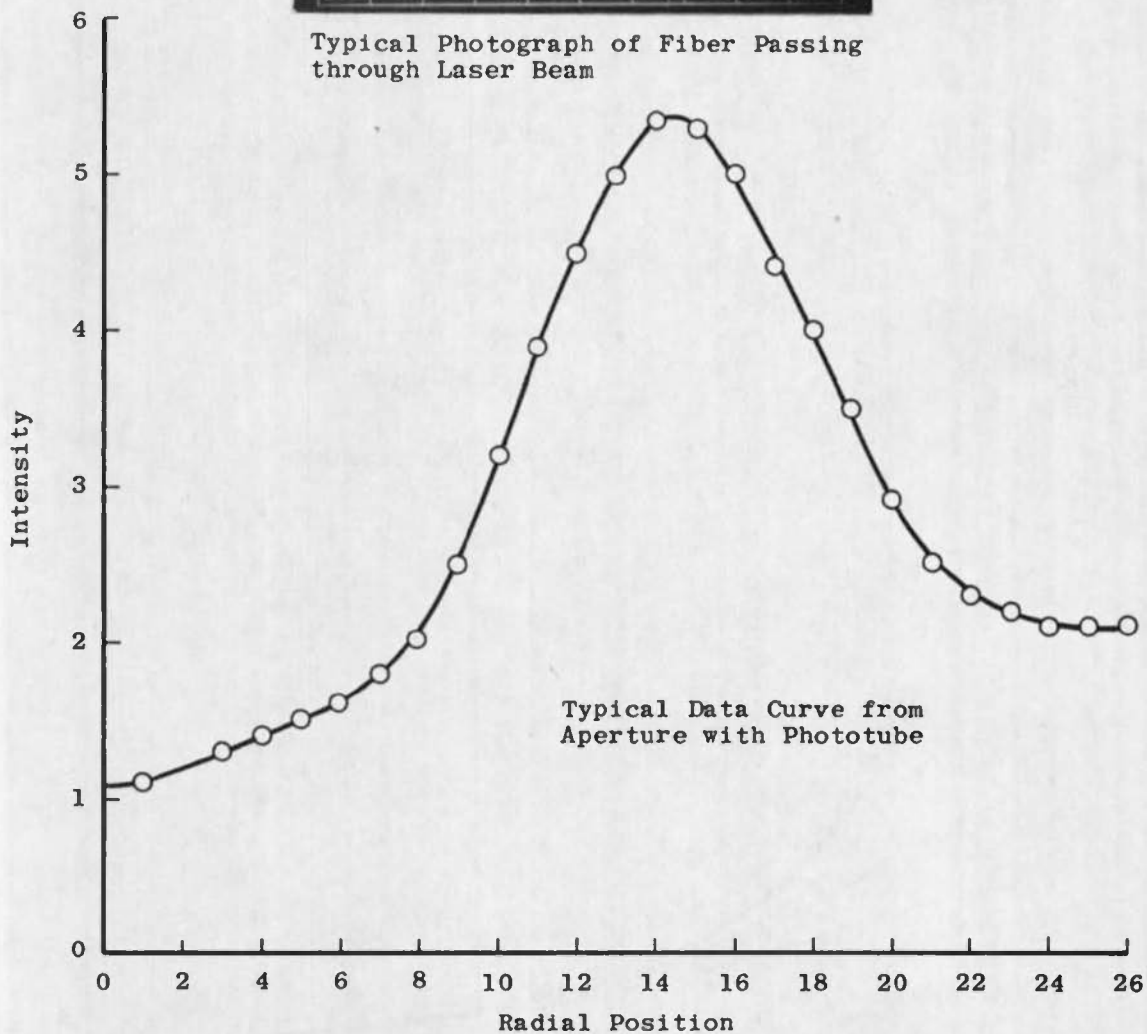


Fig. 4 Axial Intensity versus Axial Position

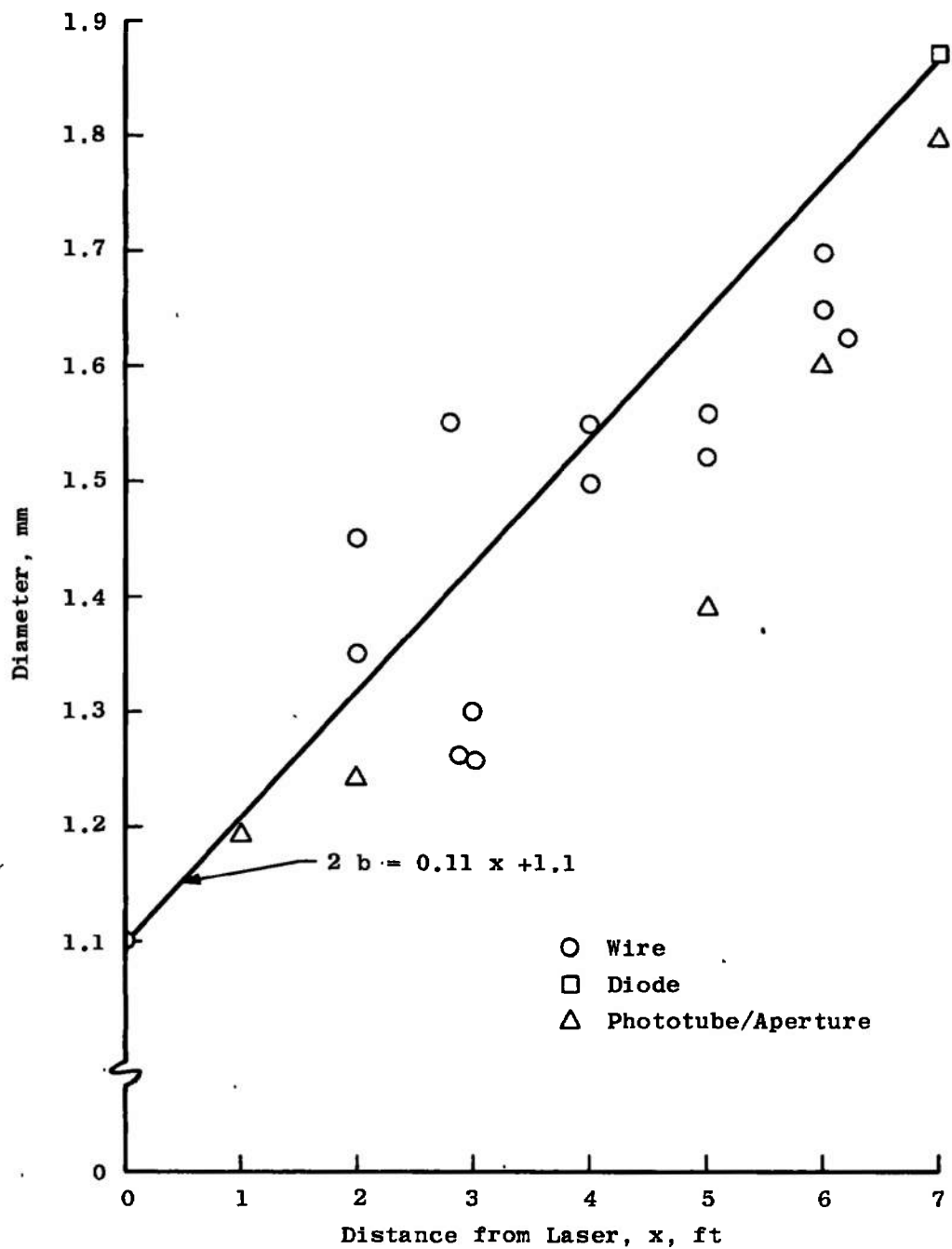
Fig. 5 Plot of the Function  $f(\phi)$  versus  $\phi$



Typical Photograph of Fiber Passing through Laser Beam

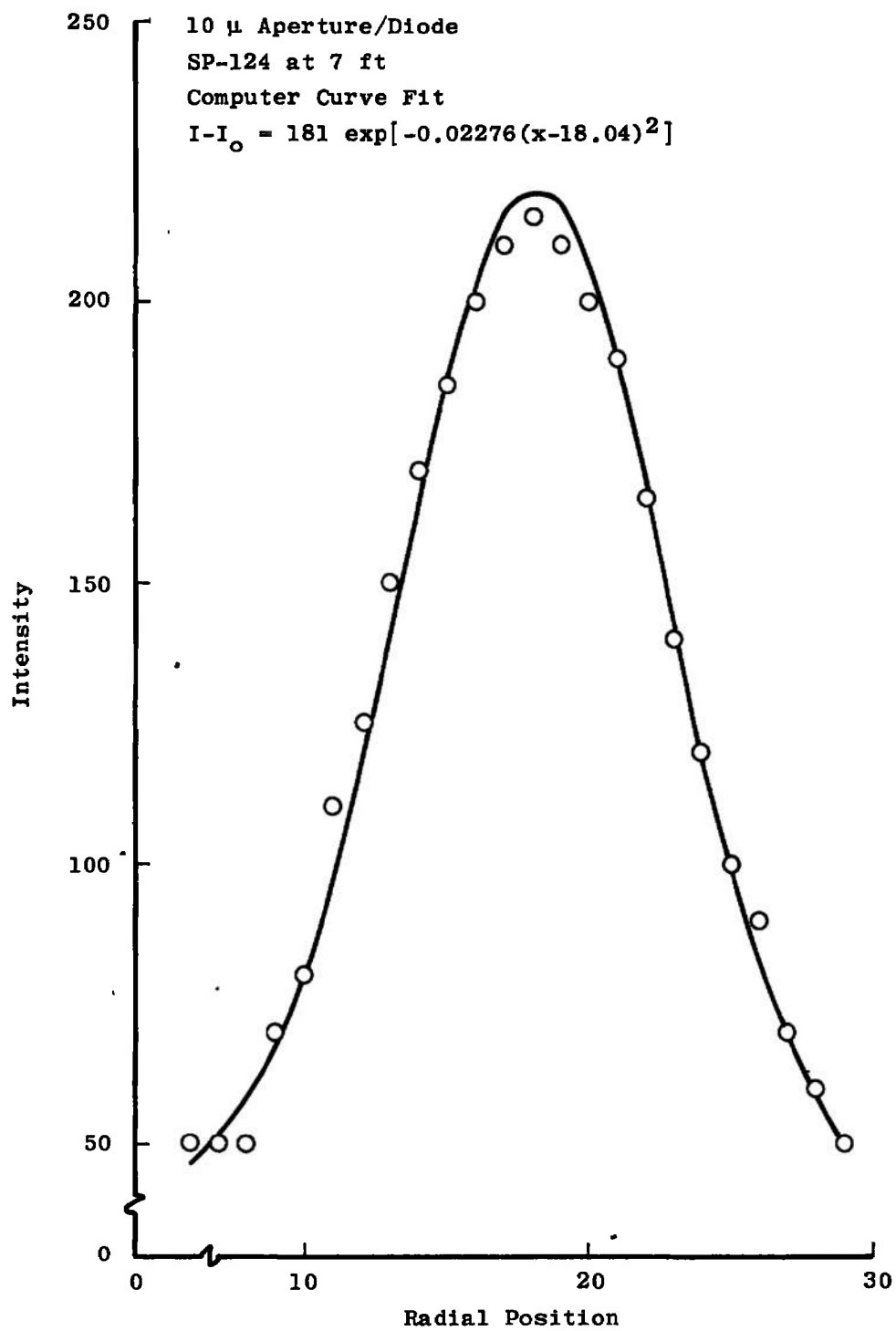


a. Representative Data of Laser Beam Intensity versus Radial Position  
Fig. 6 Typical Data Plots



b. Plot of Beam Diameter versus Distance for SP-124  
Fig. 6 Continued





c. Intensity Plot of Diode Data with Computer Curve Fit  
Fig. 6 Concluded

Automatic Diode Scan  
at 19.48 ft of Spectra  
Physics 140 Laser

$$\frac{(\text{Scan Speed})(1/2 \text{ Width}) \times 1.428}{\text{Chart Speed}} = \frac{1}{e^2} \text{ Width}$$

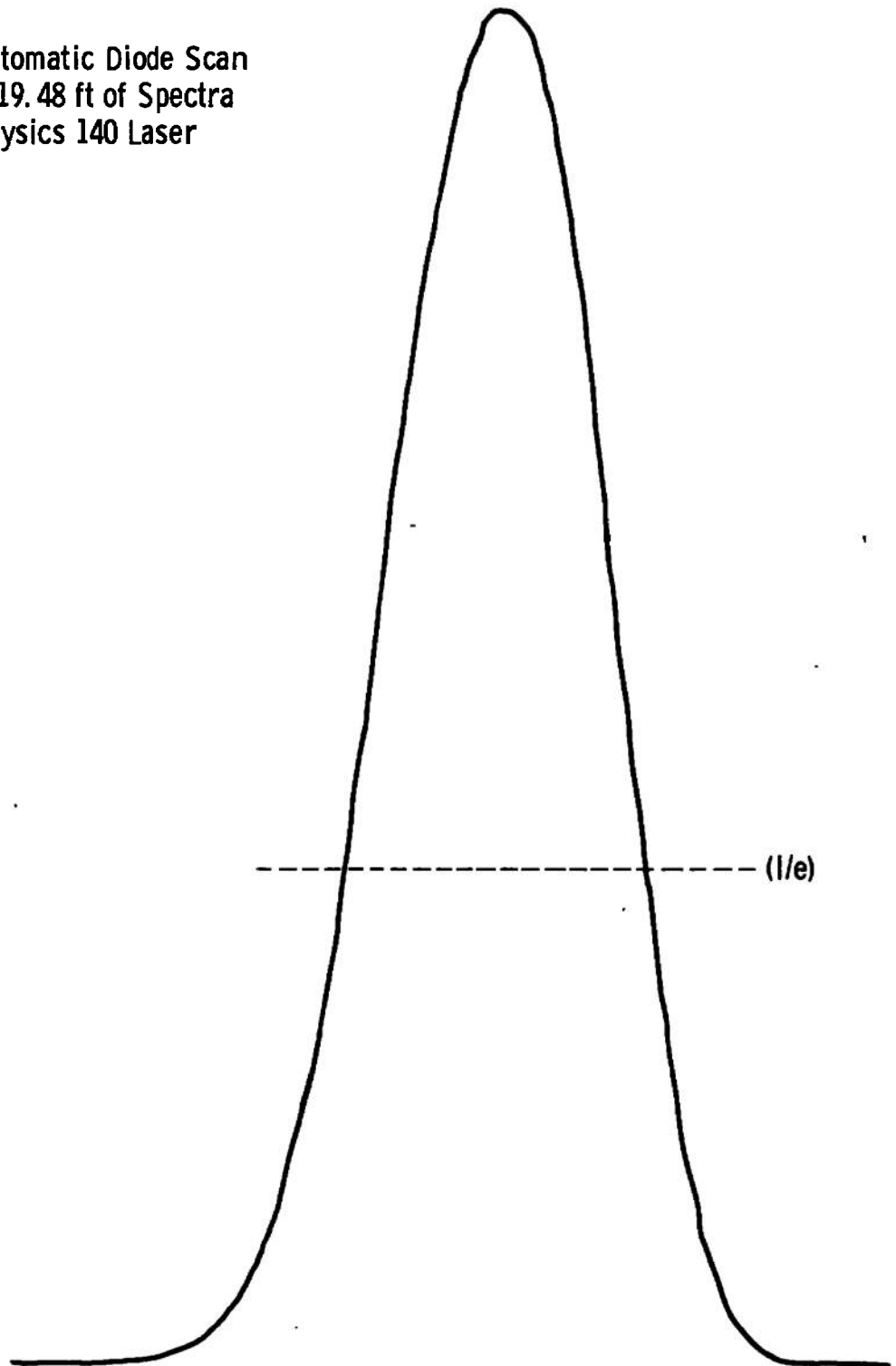


Fig. 7 Automatic Diode Scan of Laser Beam Diameter for SP-140

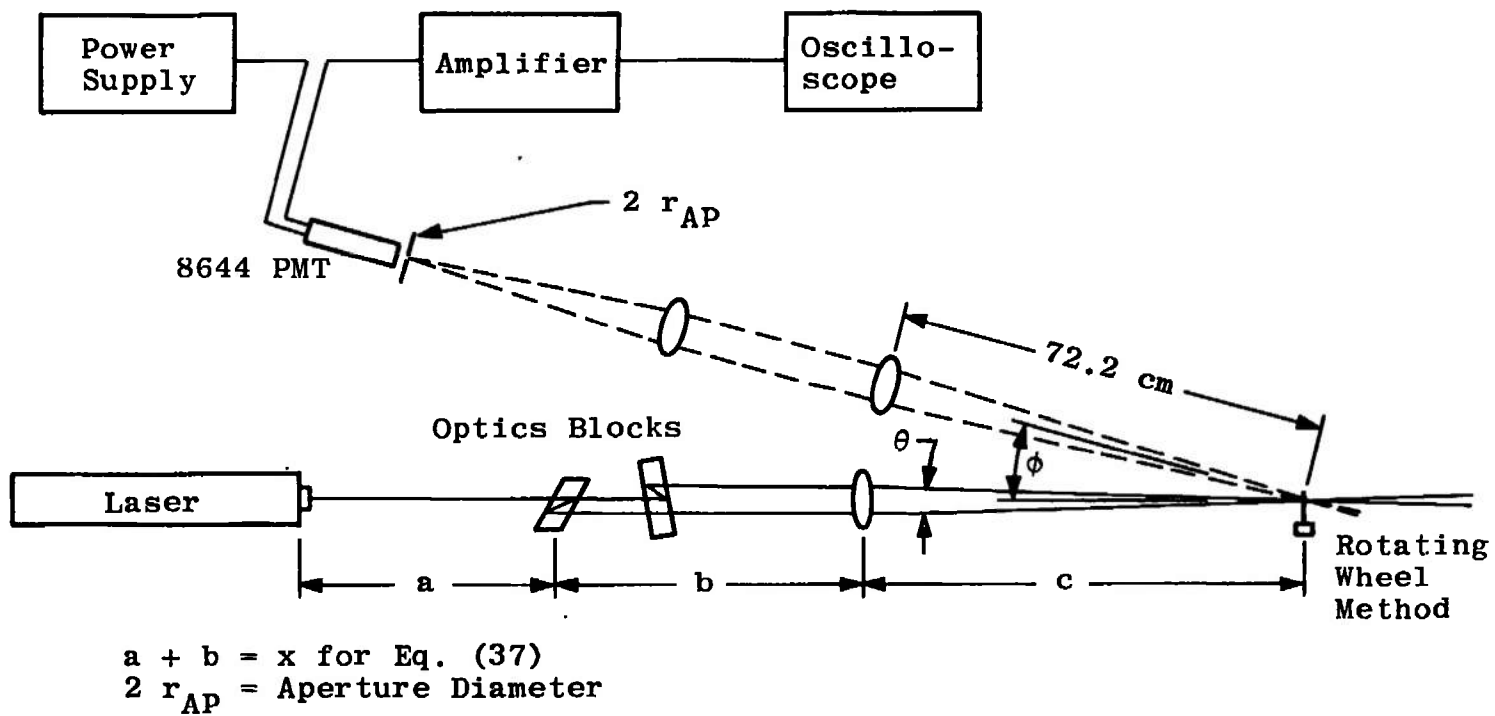


Fig. 8 Typical Setup for Off-Axis Experiments

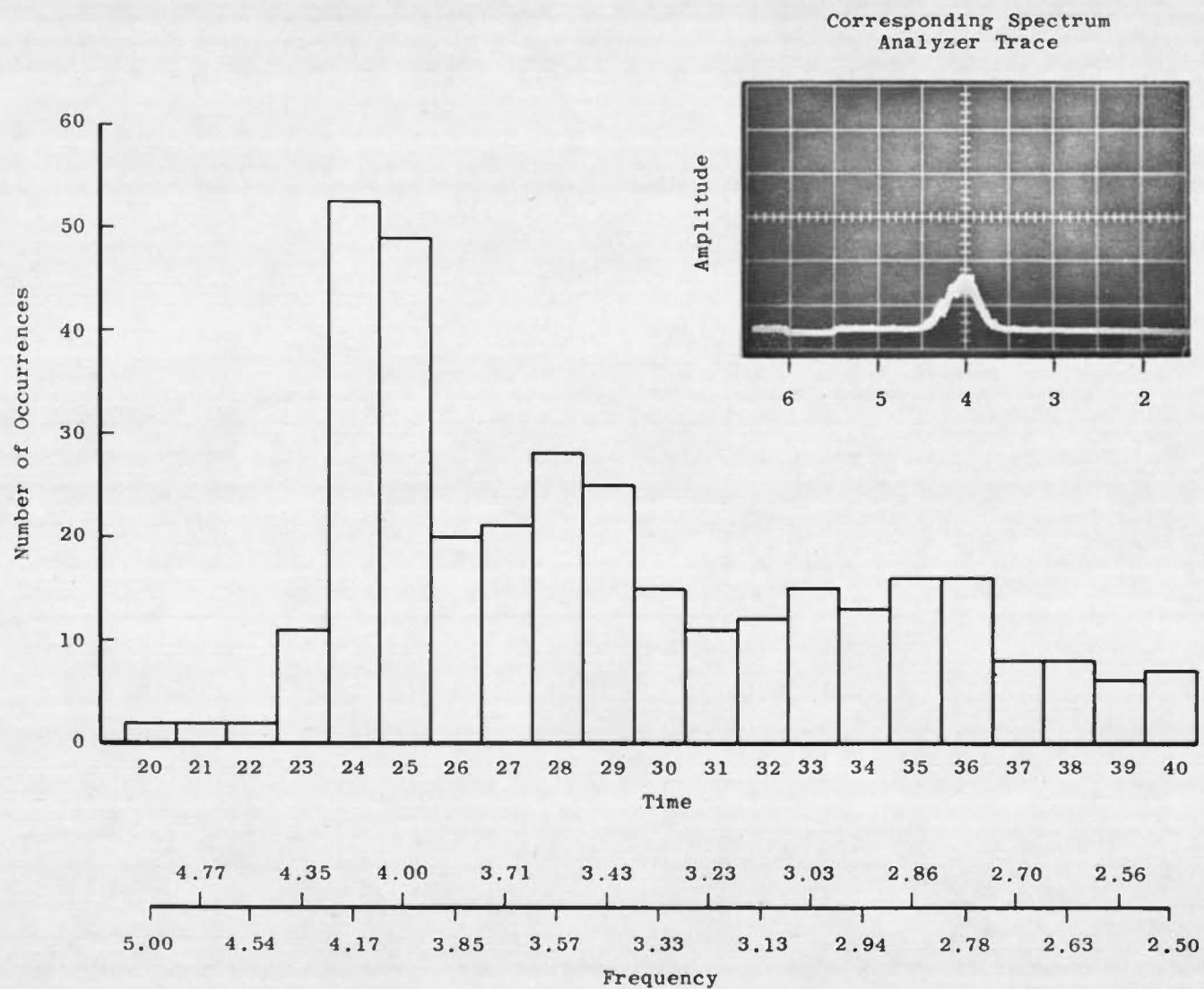


Fig. 9 Zero Crossing Electronic Readout

## APPENDIX II GAUSSIAN CURVE FITTING

Assume that experiment provides a table of the quantities  $I$  and  $x$ , and that  $I$  is known to be a Gaussian function of  $x$ ,

$$I = I_0 e^{-\frac{2(x - x_0)^2}{b^2}} \quad (\text{II-1})$$

where  $I_0$  is the maximum value of  $I$ ,  $x_0$  is the origin about which the  $x$  data are taken (only in rare cases would  $x_0 = 0$ ), and  $b$  is a constant. The constant  $b$  is useful because  $I(x = b) = I_0/e^2$  and therefore  $2b$  is a convenient measure of the "diameter" of the Gaussian function.

This appendix describes how one can determine the value of  $b$  from a table of  $I$  versus  $x$ . The method of least squares is employed.

Most computing facilities have a standard program for performing least-squares curve fits to function of the form

$$y = a_0 + a_1 x + a_2 x^2 + \dots + a_n x^n \quad (\text{II-2})$$

in which

$$y = \ln I \quad (\text{II-3})$$

$$a_0 = \ln I_0 - \frac{2x_0^2}{b^2} \quad (\text{II-4})$$

$$a_1 = \frac{4x_0}{b^2} \quad (\text{II-5})$$

and

$$a_2 = \frac{-2}{b^2} \quad (\text{II-6})$$

A table of  $I$  versus  $x$  containing  $N$  entries can be written in the matrix form

$$\begin{bmatrix} y_1 \\ y_2 \\ \vdots \\ y_n \end{bmatrix} = \begin{bmatrix} 1 & x_1 & x_1^2 \\ 1 & x_2 & x_2^2 \\ \vdots & \vdots & \vdots \\ 1 & x_n & x_n^2 \end{bmatrix} \begin{bmatrix} a_0 \\ a_1 \\ a_2 \end{bmatrix} \quad (\text{II-7})$$

or as

$$Y = XA \quad (\text{II-8})$$

The matrix A is found to be

$$A = (\tilde{X} X)^{-1} \tilde{X} Y \quad (\text{II-9})$$

The variance in y is given by

$$\sigma_y^2 = \frac{\tilde{Y}Y - \tilde{A}\tilde{X}Y}{N-1} \quad (\text{II-10})$$

and the variance-covariance matrix (the diagonal elements are the variances in the constants  $a_0$ ,  $a_1$ , and  $a_2$ ) is given by

$$V = \sigma_y^2 (\tilde{X} X)^{-1} \quad (\text{II-11})$$

In order to apply the above matrix equations, one must prepare a table of  $\ln I$  versus  $x$  from the original table of  $I$  versus  $x$ , and then write the new table in matrix notation. The matrix manipulations are then done; one finds the Gaussian diameter from Eqs. (II-9) and (II-6).

$$2b = \sqrt{\frac{-8}{a_2}} \quad (\text{II-12})$$

The standard deviation in the diameter is given by

$$\begin{aligned} \sigma(2b) &= \frac{\sqrt{2}}{a^{3/2}} \sigma(a_2) \\ &= \frac{-b^3 \sigma(a_2)}{2} \end{aligned} \quad (\text{II-13})$$

where  $\sigma(a_2)^2$  is the appropriate element of the variance-covariance matrix V.

## DOCUMENT CONTROL DATA - R &amp; D

(Security classification of title, body of abstract and indexing annotation must be entered when the overall report is classified)

|   |  |  |                     |
|---|--|--|---------------------|
| 1. ORIGINATING ACTIVITY (Corporate author)<br>Arnold Engineering Development Center<br>ARO, Inc., Operating Contractor<br>Arnold Air Force Station, Tennessee 37389 |  | 2a. REPORT SECURITY CLASSIFICATION<br>UNCLASSIFIED   |                     |
|   |  | 2b. GROUP<br>N/A   |                     |
| 3. REPORT TITLE<br>LASER DOPPLER VELOCIMETER DUAL SCATTER PROBE VOLUME  |  |  |                     |
| 4. DESCRIPTIVE NOTES (Type of report and inclusive dates)<br>Final Report - July through October 1970   |  |  |                     |
| 5. AUTHOR(S) (First name, middle initial, last name)<br>W. H. Goethert, ARO, Inc.   |  |  |                     |
| 6. REPORT DATE<br>July 1971   |  | 7a. TOTAL NO OF PAGES<br>39  | 7b. NO OF REFS<br>4 |
| 8a. CONTRACT OR GRANT NO<br>F40600-72-C-0003  |  | 9a. ORIGINATOR'S REPORT NUMBER(S)<br>AEDC-TR-71-85   |                     |
| b. PROJECT NO 4344  |  | 9b. OTHER REPORT NO(S) (Any other numbers that may be assigned this report)<br>ARO-OMD-TR-71-24                                      |                     |
| c. Task 32  |  |  |                     |
| d. Program Element 65701F   |  |  |                     |
| 10. DISTRIBUTION STATEMENT<br>Approved for public release; distribution unlimited.  |  |  |                     |
| 11. SUPPLEMENTARY NOTES<br>Available in DDC   |  | 12. SPONSORING MILITARY ACTIVITY<br>Arnold Engineering Development Center, Air Force Systems Command, Arnold AF Station, Tenn. 37389 |                     |

13. ABSTRACT

A further clarification of the volume from which data originate in the dual scatter laser Doppler velocimeter is presented. There are several factors that specify the primary dimensions of the probe volume which in some cases are totally specified by the collector optics. It was found experimentally that the lens aperture of the light collecting optics has a primary effect on the volume from which data originate. An equation is derived for reducing this data volume for both the on-axis and off-axis cases. Experimental verification is presented and compared to the derived equation.

14.

## KEY WORDS

speed indicators

lasers

doppler effect

detectors

wind tunnels

## LINK A

## LINK B

## LINK C

ROLE

WT

ROLE

WT

ROLE

WT